JACS
JOURNAL OF THE AMERICAN CHEMICAL SOCIETY

Communication

pubs.acs.org/JACS

Supramolecular Switching between Flat Sheets and Helical Tubules Triggered by Coordination Interaction

Suyong Shin, Sunhee Lim, Yongju Kim,* Taehoon Kim, Tae-Lim Choi, and Myongsoo Lee*

Department of Chemistry, Seoul National University, Seoul 151-747, Korea

Supporting Information

ABSTRACT: Here we report the spontaneous formation of switchable sheets in aqueous solution, which is based on bent-shaped aromatic amphiphiles containing *m*-pyridine units at the terminals and a hydrophilic dendron at the apex. The aromatic segments self-assemble into flat sheets consisting of a zigzag conformation through $\pi-\pi$ stacking interactions. Notably, the sheets reversibly transform into helical tubules at higher concentration and into discrete dimeric macrocycles at a lower concentration in response to Ag(I) ions through reversible coordination interactions between the pyridine units of the aromatic segments and the Ag(I) ions. While maintaining the coordination bonding interactions, the helical tubules reversibly transform into the dimeric macrocycles in response to the variation in concentration.

The spontaneous assembly of small molecular modules by the orchestrated interplay of various non-covalent interactions is a challenging research topic in the field of supramolecular chemistry.[1] The reversibility of such non-covalent interactions opens up interesting applications to direct the systems toward the formation of dynamic architectures with responsive functions.[2] Rigid-rod amphiphiles consisting of hydrophobic aromatic and hydrophilic coil segments have been proven to be promising scaffolds for switchable superstructures in response to external forces.[2b,3] For example, dumbbell-shaped aromatic rods grafted to hydrophilic oligoether dendrons aggregate to form porous capsules with gated lateral pores in response to changing temperature.[4] Lateral attachment of dendritic segments into an aromatic rod leads the molecules to self-assemble into foldable sheets that spontaneously roll up into scrolled tubules.[5] We recently reported that synthetic tubules can be constructed by self-assembly of bent-shaped aromatic building blocks containing an oligoether dendron at the apex.[6] The bent-shaped rigid segments with an internal angle of 120° fit together easily to form non-covalent hexameric macrocycles that have flexible diameters because of the sliding motions between the molecules, creating dynamic tubules.[7] Increasing the strength of the aromatic interactions of the rigid building blocks causes non-covalent macrocycles based on a cisoid stacking pattern to transform into two-dimensional (2D) layers based on a fully overlapped zigzag packing arrangement.[8]

We envisioned that the introduction of meta-linked pyridine units at both ends of the bent-shaped aromatic segment might form stimuli-responsive 2D structures, since pyridine units are well-known to interact specifically with Ag(I) ions through reversible coordination bonds.[9] This recognition event would cause reversible rearrangement of the fully overlapped zigzag packing arrangement of the bent-shaped rigid segments to maximize the coordination interactions between pyridine donors and Ag(I) ions at the expense of $\pi-\pi$ stacking interactions between aromatic rod segments.[10] Consequently, this metal-directed rearrangement of the aromatic segments would endow the 2D structures with dynamic responsive functions. With this direction of research in mind, we synthesized self-assembling molecules **1** and **2** consisting of a long bent-shaped aromatic segment containing *m*-pyridine units at both ends and a hydrophilic oligoether dendron with an *S* configuration grafted at the apex. Here we report their spontaneous self-assembly to form responsive 2D sheets in aqueous solution (Figure 1). Notably, these 2D sheets reversibly transform into hollow tubules with helical cavities through a cyclic conformation of the aromatic segments in response to Ag(I) ions (see Figure 5).

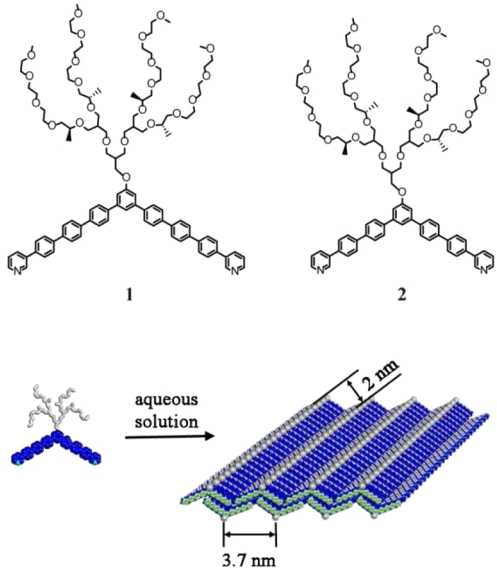

Figure 1. Molecular structures of bent-shaped amphiphiles **1** and **2** and schematic representation of the formation of responsive 2D sheets with a fully overlapped zigzag conformation of the bent-shaped aromatic segments in aqueous solution.

Received: January 7, 2013
Published: January 28, 2013

ACS Publications © 2013 American Chemical Society

dx.doi.org/10.1021/ja400160j | J. Am. Chem. Soc. 2013, 135, 2156−2159

The aromatic amphiphiles were synthesized starting with Suzuki coupling of a 2,6-dibromophenol derivative with trimethylsilyl (TMS)-protected phenylboronic acid. The resulting compound was subjected to an etherification reaction with an oligoether dendritic chain. The transformation of the TMS groups to iodo groups was achieved by iodination with ICl. Suzuki couplings of the diiodo compound with TMS-substituted biphenylboronoic acid and TMS-substituted phenylboronic acid were used to prepare the precursors of **1** and **2**, respectively. The final compounds were successfully synthesized by Suzuki coupling with 3-pyridylboronic acid. The resulting molecules were characterized by ^{1}H and ^{13}C NMR spectroscopies and MALDI-TOF mass spectroscopy and shown to be in full agreement with the structures presented.

Molecule **1** self-assembles into flat sheets in dilute aqueous solutions. Cryogenic transmission electron microscopy (cryo-TEM) showed sheetlike objects with curved edges against the vitrified solution background (Figure 2a), indicative of the formation of flexible sheets in bulk solution. To obtain more information on these sheets, we additionally performed TEM experiments with samples cast onto a TEM grid and negatively stained with uranyl acetate. The image shows planar sheets with regular stripes having a periodicity of 2 nm against a dark background (Figure 2b inset). This result suggests that the aromatic segments with a zigzag conformation are oriented parallel to the sheet plane, similar to the organization in the layered structures of bent-shaped molecules.[8] The interapex distance of 3.7 nm within the zigzag conformation, as obtained from molecular modeling, indicates that the adjacent aromatic segments are slipped relative to each other with an angle of 57.4° to release the steric hindrance between the bulky dendritic chains (Figure 1).

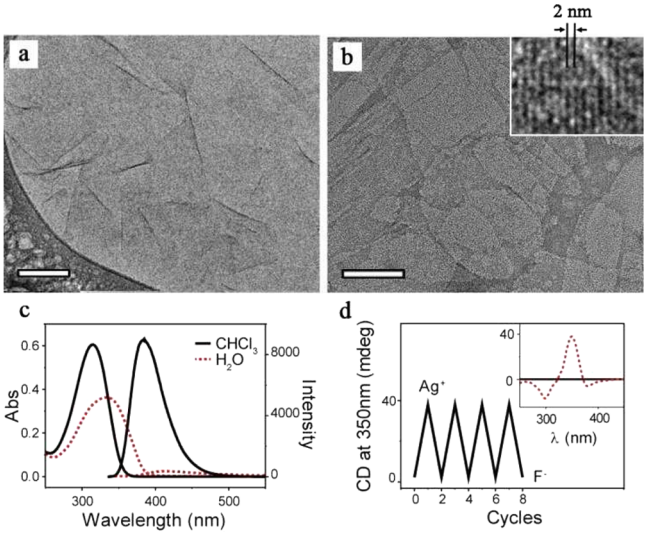

Figure 2. (a) Cryo-TEM image and (b) negative-stain TEM image of **1** obtained from a 0.03 wt % aqueous solution (scale bars = 100 nm). The inset is a magnified image of (b). (c) Absorption and emission spectra of **1** (0.03 wt %) in $CHCl_3$ solution (solid black lines) and aqueous solution (dotted red lines); λ_{ex} = 315 and 333 nm, respectively. (d) Reversible CD signal changes at λ_{max} = 350 nm for an aqueous solution of **1** (0.03 wt %) upon cycles of complexation and subsequent decomplexation. The inset shows CD spectra of an aqueous solution of **1** (0.03 wt %) without Ag(I) ions (solid black line) and with Ag(I) ions (dotted red line).

Optical spectroscopy investigation of **1** displayed that the absorption maximum in aqueous solution is red-shifted and the fluorescence intensity significantly quenched with respect to those observed in chloroform solutions, indicative of the formation of aqueous aggregates through $\pi-\pi$ interactions of the aromatic segments (Figure 2c).[3a,11] When molecule **1** in aqueous solution was subjected to circular dichroism (CD) measurements, no CD signals could be detected, as would be expected for symmetric 2D objects, even though **1** contains chiral side groups (Figure 2d). To investigate the effect of the length of the aromatic segments for the 2D sheets, we also investigated **2**, an analogue of **1** with shorter aromatic segments. In great contrast to **1**, **2** did not show any aggregation behavior in aqueous solution even at high concentrations.

The formation of flat sheets with a pyridine interior suggested that **1** in aqueous solution would exhibit Ag(I) ion-responsive behavior because the pyridine units would interact with Ag(I) ions through coordination bonds.[9] This interaction was confirmed by ^{1}H NMR measurements for **1** upon the addition of 1 molar equivalent of silver triflate (Figure S1 in the Supporting Information). The proton resonances associated with the pyridine units were considerably shifted downfield, demonstrating that the Ag(I) ions were coordinated to the pyridine units of the aromatic segments.[12] Remarkably, addition of the silver salt to the solution of **1** at a concentration of 0.03 wt % induced significant CD signals (Figure 2d), suggesting that the 2D structures transformed into chiral superstructures. The CD signals immediately disappeared upon decomplexation by the addition of tetra-*n*-butylammonium fluoride (Bu_4NF),[13] indicating that this transformation is reversible over many cycles (Figure 2d).

The structural transformation of the 2D structure upon the addition of Ag(I) ions was visualized by TEM (Figure 3a).

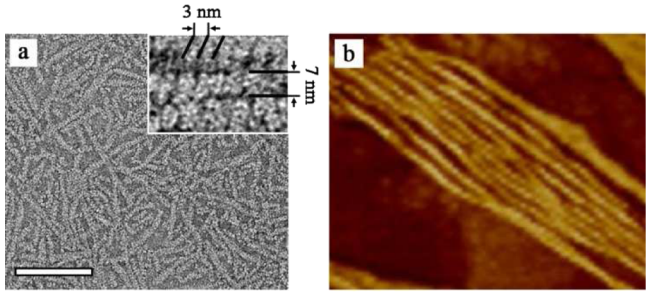

Figure 3. (a) TEM image (scale bar = 200 nm; the inset is a magnified image) and (b) AFM image (450 nm × 350 nm) of an aqueous solution of **1** with Ag(I) ions (0.03 wt %).

When the sample was cast from the solution and then negatively stained with uranyl acetate, the image showed undulated helical objects with a uniform diameter of 7 nm and a left-handed helical sense with a pitch of 3 nm. To corroborate further the handedness of the helical objects, we performed atomic force microscopy (AFM) experiments on a SiO_2/Si wafer in a completely dried state. The images revealed bundles of rodlike aggregates with a diameter of ~10 nm, which is larger than the value determined from TEM (Figure 3b). This difference could in part arise from deformation of the rodlike objects on the wafer surface. Closer examination of the image (Figure 3b) revealed a left-handed helical structure with a

dx.doi.org/10.1021/ja400160j | J. Am. Chem. Soc. 2013, 135, 2156−2159

regular pitch along the rod axis, which is consistent with the result obtained from TEM.

The question arose in this step whether the helical structures were based on helical folding of the coordination-bonded polymeric chains or helical stacking of metal-mediated aromatic macrocycles. To answer this question, we performed dynamic light scattering (DLS) experiments using diluted solutions of **1** with decreasing concentration (Figure 4a). As the concentration decreased from 0.03 to 0.01 wt %, the size (hydrodynamic diameter) abruptly decreased from 200 to 8 nm, suggesting that the helical objects originated from helical stacking of small objects rather than helical folding of polymeric chains. When the diluted solution with a concentration of 0.01 wt % was subjected to TEM measurements, uniform toroidal structures were observed (Figure 4c). The electron density profile showed that the external diameter and the diameter of the internal cavity of the toroid were 7 and 2.5 nm, respectively. To provide further confirmation of the formation of the toroids, we performed AFM measurements on samples prepared by drop-casting of the 0.01 wt % aqueous solution onto the SiO_2/Si wafer (Figure 4d). The image clearly revealed toroidal objects with a height of 4 Å, demonstrating that the toroidal objects were single stacks of these macrocycles.

To gain further insight into the toroidal structure, we conducted vapor pressure osmometry (VPO) measurements in tetrahydrofuran solution over the concentration range 8.5−17.0 g/kg (sample/solvent). The molecular weight of the primary aggregate was measured to be 3902 Da, which is 2 times larger than that of a single molecule containing a silver ion (1894 Da) (Figure S3), indicating the metal-containing dimeric association. All of these observations, together with inspection of Corey−Pauling−Koltun (CPK) models, indicate that **1** self-assembles into dimeric macrocycles formed through coordination bonding interactions between pyridines and Ag(I) ions under diluted conditions at a concentration of 0.01 wt % (Figure 4e).

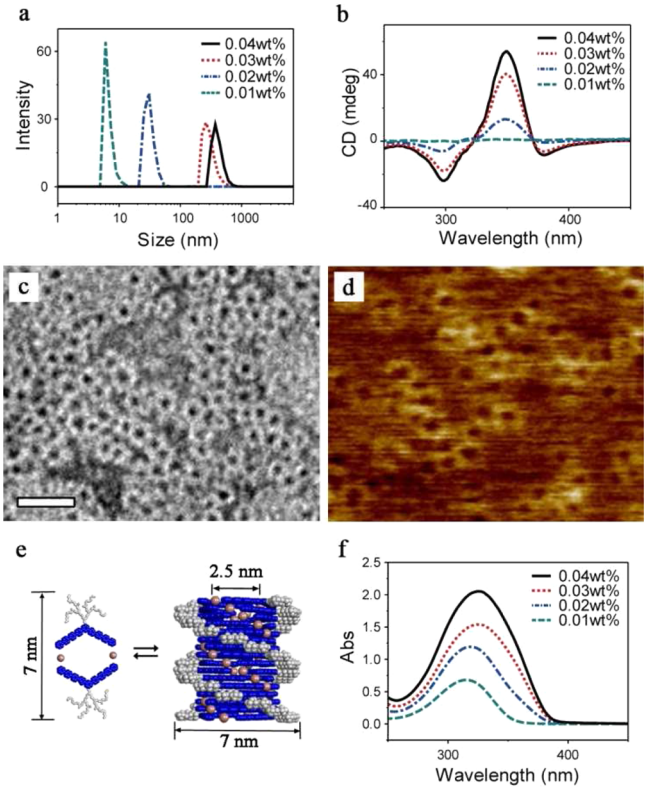

Figure 4. (a) Size distribution from DLS measurements and (b) CD spectra of aqueous solutions of **1** with Ag(I) ions at decreasing concentrations from 0.04 to 0.01 wt %. (c) TEM image (scale bar = 25 nm) and (d) AFM image (250 nm × 200 nm) of aqueous solution of **1** with Ag(I) ions (0.01 wt %). (e) Schematic representation of the switch between Ag(I) ion-mediated dimeric macrocyclic structure and the tubular structure. (f) UV spectra of **1** with Ag(I) ions in aqueous solution at various concentrations.

On the basis of these results, it can be concluded that the helical objects observed for a complex solution with a concentration of 0.03 wt % consisted of helical stacks of Ag(I) ion-mediated dimeric macrocycles that resulted in a tubular structure with an external diameter of 7 nm and an internal cavity diameter of 2.5 nm (Figure 4e). The formation of tubules based on helical stacks of the macrocycles is also reflected in the preservation of the external dimension of the macrocycle, which was essentially unaltered relative to that of the helical objects even after the concentration was increased. CD spectra showed increased intensity with increasing concentration (Figure 4b), indicative of helical stacking of the macrocycles with a preferred handedness, which is consistent with the results observed by TEM and AFM. This result demonstrates that the primary dimeric macrocycles stack on top of each other with mutual rotation in the same direction. Consequently, this helically staggered stacking of the dimeric macrocycles leads to a tubular structure with a left-handed supramolecular chirality (Figure 4e).

The results described here demonstrate that Ag(I) ions trigger drastic supramolecular switching between nonchiral flat sheets and helical tubules with supramolecular chirality (Figure 5). This structural transformation originates from the dissociation of the zigzag polymer chains through a breakup of the $\pi-\pi$ stacking interactions upon the addition of silver salt to form discrete dimeric macrocycles mediated by strong coordination bonding interactions.[10] The breakup of the $\pi-\pi$ stacking interactions upon the addition of silver salt is manifested in the blue shift of the absorption maximum (λ_{max} = 315 nm) relative to that of the dilute solution of **1** at a concentration of 0.01 wt % (λ_{max} = 333 nm).[3] This blue shift of the absorption maximum (λ_{max} = 325 to 315 nm) was also observed with decreasing concentration of the Ag(I) complex solution (Figure 4f), indicating the absence of $\pi-\pi$ stacking

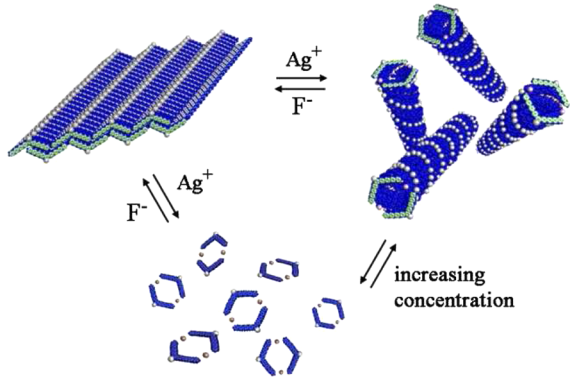

Figure 5. Schematic representation of reversible transformation through flat sheets, helical tubules and discrete toroids in response to external stimuli.

dx.doi.org/10.1021/ja400160j | J. Am. Chem. Soc. 2013, 135, 2156−2159

interactions under dilute conditions at a concentration of 0.01 wt %. It should be mentioned that the blue-shifted absorption maximum was also observed for the molecularly dissolved state in $CHCl_3$ solution (Figure 2c). When Bu_4NF was added to break the coordination bond interactions through decomplexation, the absorption maximum was red-shifted to recover that of the solution of **1**, indicating that the decomplexed aromatic segments reassemble into the sheets through $\pi-\pi$ stacking interactions, as confirmed by TEM.

On the basis of all of the data described here, the sheets can be considered to undergo a drastic transformation into helical tubules at a higher concentration and a transformation into discrete dimeric macrocycles at a lower concentration through reversible coordination interactions between the pyridine units of the aromatic segments and Ag(I) ions (Figure 5). Another interesting point to be noted is that the metal-containing macrocycles reversibly stack on top of each other to form helical tubules in response to a variation in the concentration. The primary driving force responsible for the metal-directed switching behavior of the sheets is the dominant coordination interactions between the pyridine units of the aromatic segments and Ag(I) ions, which overcome the weak stacking interactions of the aromatic segments. This interplay of different non-covalent interactions allows the 2D structures to be transformed immediately into helical or macrocyclic structures depending on the concentration.

In conclusion, we have demonstrated that stimuli-responsive 2D structures can be constructed by the aqueous self-assembly of bent-shaped aromatic rods containing pyridine units at their terminals. The sheets respond to Ag(I) ions by changing their shape into helical tubules at a higher concentration and discrete macrocycles at a lower concentration. It is worth noting that the metal-containing macrocycles reversibly stack on top of each other to form helical tubules in response to the variation in concentration. In comparison with conventional fixed 2D structures,[14] the most notable feature of our systems is their ability to respond to external stimuli by a direct structural change from nonchiral flat 2D structures to 1D hollow structures with helical pores. Such a unique switch of the open sheets into closed tubules with helical pores opens up the new possibility of using the 2D structures to capture specific proteins selectively in their helical interior and release them to their target.

■ ASSOCIATED CONTENT

Ⓢ Supporting Information

Experimental procedures; synthetic method; NMR, MALDI-TOF, and VPO data; and a TEM image. This material is available free of charge via the Internet at http://pubs.acs.org.

■ AUTHOR INFORMATION

Corresponding Author

yongju00@snu.ac.kr; myongslee@snu.ac.kr

Notes

The authors declare no competing financial interest.

■ ACKNOWLEDGMENTS

This material is based on research sponsored by the Air Force Research Laboratory under Agreement FA2386-12-1-4078. We thank Prof. Z. Huang (HIT) for his valuable input with molecular synthesis.

■ REFERENCES

(1) (a) Aida, T.; Meijer, E. W.; Stupp, S. I. *Science* **2012**, *335*, 813. (b) De Greef, T. F. A.; Smulders, M. M. J.; Wolffs, M.; Schenning, A. P. H. J.; Sijbesma, R. P.; Meijer, E. W. *Chem. Rev.* **2009**, *109*, 5687. (c) Shimizu, T.; Masuda, M.; Minamikawa, H. *Chem. Rev.* **2005**, *105*, 1401. (d) Ajayaghosh, A.; Praveen, V. K. *Acc. Chem. Res.* **2007**, *40*, 644. (e) Rosen, B. M.; Wilson, C. J.; Wilson, D. A.; Peterca, M.; Imam, M. R.; Percec, V. *Chem. Rev.* **2009**, *109*, 6275.

(2) (a) Yagai, S.; Kinoshita, T.; Kikkawa, Y.; Karatsu, T.; Kitamura, A.; Honsho, Y.; Seki, S. *Chem.—Eur. J.* **2009**, *15*, 9320. (b) Kim, H.-J.; Kim, T.; Lee, M. *Acc. Chem. Res.* **2010**, *44*, 72. (c) Shao, H.; Parquette, J. R. *Angew. Chem., Int. Ed.* **2009**, *48*, 2525. (d) Goto, H.; Furusho, Y.; Yashima, E. *J. Am. Chem. Soc.* **2007**, *129*, 109. (e) Gopal, A.; Hifsudheen, M.; Furumi, S.; Takeuchi, M.; Ajayaghosh, A. *Angew. Chem., Int. Ed.* **2012**, *51*, 10505. (f) Ajayaghosh, A.; Chithra, P.; Varghese, R. *Angew. Chem., Int. Ed.* **2007**, *46*, 230. (g) Yagai, S.; Kubota, S.; Saito, H.; Unoike, K.; Karatsu, T.; Kitamura, A.; Ajayaghosh, A.; Kanesato, M.; Kikkawa, Y. *J. Am. Chem. Soc.* **2009**, *131*, 5408. (h) Palmans, A. R. A.; Meijer, E. W. *Angew. Chem., Int. Ed.* **2007**, *46*, 8948. (i) Sim, S.; Kim, Y.; Kim, T.; Lim, S.; Lee, M. *J. Am. Chem. Soc.* **2012**, *134*, 20270. (j) Yan, Y.; Wang, H.; Li, B.; Hou, G.; Yin, Z.; Wu, L.; Yam, V. W. *Angew. Chem., Int. Ed.* **2010**, *49*, 9233. (k) Chen, S.; Chen, L.-J.; Yang, H.-B.; Tian, H.; Zhu, W. *J. Am. Chem. Soc.* **2012**, *134*, 13596. (l) Lu, X.; Guo, Z.; Sun, C.; Tian, H.; Zhu, W. *J. Phys. Chem. B* **2011**, *115*, 10871.

(3) (a) Ryu, J.-H.; Hong, D.-J.; Lee, M. *Chem. Commun.* **2008**, 1043. (b) Huang, Z.; Kang, S.-K.; Lee, M. *J. Mater. Chem.* **2011**, *21*, 15327. (c) Huang, Z.; Lee, H.; Lee, E.; Kang, S.-K.; Nam, J.-M.; Lee, M. *Nat. Commun.* **2011**, *2*, 459.

(4) Kim, J.-K.; Lee, E.; Lim, Y.-b.; Lee, M. *Angew. Chem., Int. Ed.* **2008**, *47*, 4662.

(5) Lee, E.; Kim, J.-K.; Lee, M. *Angew. Chem., Int. Ed.* **2009**, *48*, 3657.

(6) Kim, H.-J.; Kang, S.-K.; Lee, Y.-K.; Seok, C.; Lee, J.-K.; Zin, W.-C.; Lee, M. *Angew. Chem., Int. Ed.* **2010**, *122*, 8649.

(7) Huang, Z.; Kang, S.-K.; Banno, M.; Yamaguchi, T.; Lee, D.; Seok, C.; Yashima, E.; Lee, M. *Science* **2012**, *337*, 1521.

(8) Kim, H.-J.; Liu, F.; Ryu, J.-H.; Kang, S.-K.; Zeng, X.; Ungar, G.; Lee, J.-K.; Zin, W.-C.; Lee, M. *J. Am. Chem. Soc.* **2012**, *134*, 13871.

(9) (a) Khlobystov, A. N.; Blake, A. J.; Champness, N. R.; Lemenovskii, D. A.; Majouga, A. G.; Zyk, N. V.; Schröder, M. *Coord. Chem. Rev.* **2001**, *222*, 155. (b) Yue, N. L. S.; Jennings, M. C.; Puddephatt, R. J. *Dalton Trans.* **2010**, *39*, 1273.

(10) (a) Wilkinson, G.; Gillard, R. D.; McCleverty, J. A. *Comprehensive Coordination Chemistry: The Synthesis, Reactions, Properties and Applications of Coordination Compounds*; Pergamon Press: Oxford, U.K., 1987. (b) Zhang, J.; Moore, J. S. *J. Am. Chem. Soc.* **1992**, *114*, 9701. (c) Paliwal, S.; Geib, S.; Wilcox, C. S. *J. Am. Chem. Soc.* **1994**, *116*, 4497.

(11) Bae, J.; Choi, J.-H.; Yoo, Y.-S.; Oh, N.-K.; Kim, B.-S.; Lee, M. *J. Am. Chem. Soc.* **2005**, *127*, 9668.

(12) Kilpin, K. J.; Gower, M. L.; Telfer, S. G.; Jameson, G. B.; Crowley, J. D. *Inorg. Chem.* **2011**, *50*, 1123.

(13) Kim, H.-J.; Lee, J.-H.; Lee, M. *Angew. Chem., Int. Ed.* **2005**, *44*, 5810.

(14) (a) Martinek, T. A.; Hetényi, A.; Fülöp, L.; Mándity, I. M.; Tóth, G. K.; Dékány, I.; Fülöp, F. *Angew. Chem., Int. Ed.* **2006**, *45*, 2396. (b) Moon, K.-S.; Lee, E.; Lim, Y.-b.; Lee, M. *Chem. Commun.* **2008**, 4001. (c) Nam, K. T.; Shelby, S. A.; Choi, P. H.; Marciel, A. B.; Chen, R.; Tan, L.; Chu, T. K.; Mesch, R. A.; Lee, B. C.; Connolly, M. D.; Kisielowski, C.; Zuckermann, R. N. *Nat. Mater.* **2010**, *9*, 454. (d) Tang, Z.; Zhang, Z.; Wang, Y.; Glotzer, S. C.; Kotov, N. A. *Science* **2006**, *314*, 274. (e) Kim, J.-K.; Lee, E.; Jeong, Y.-H.; Lee, J.-K.; Zin, W.-C.; Lee, M. *J. Am. Chem. Soc.* **2007**, *129*, 6082.